# Single-lossy-nanoparticle sensor with a dissipatively coupled photonic molecule

Zhao-Hui Peng,[1,2,*] Chun-Xia Jia,[1,2] Yu-Qing Zhang,[1,2] Ying Yang,[1,2] and Le-Man Kuang[3,4,†]

[1]*Institute of Modern Physics and Department of Physics, College of Physics and Electronic Science, Hunan University of Science and Technology, Xiangtan 411201, China*

[2]*Hunan Provincial Key Laboratory of Intelligent Sensors and Advanced Sensor Materials, Xiangtan 411201, China*

[3]*Key Laboratory of Low-Dimension Quantum Structures and Quantum Control of Ministry of Education, Synergetic Innovation Center for Quantum Effects and Applications, and Department of Physics, Hunan Normal University, Changsha 410081, China*

[4]*Synergetic Innovation Academy for Quantum Science and Technology, Zhengzhou University of Light Industry, Zhengzhou 450002, China*

(Received 3 March 2023; accepted 28 August 2023; published 26 September 2023)

An ultrasensitive optical whispering-gallery mode (WGM) sensor is highly desirable for detecting nanoparticles and has been widely used in human disease diagnosis and environment monitoring. The sensing mechanisms of a WGM sensor include mode shift, mode splitting, and mode broadening. To enhance mode broadening is a quite useful way to improve the sensitivity for detecting lossy nanoparticles, but it has not been realized. Here, we propose a feasible scheme for realizing a single-lossy-nanoparticle sensor with a dissipatively coupled photonic molecule and show that the significant enhancement of mode broadening can be obtainable at exceptional points when compared with a single-microcavity sensor subject to the same perturbation. The enhancement of mode broadening originates from the complex-square-root topology near exceptional points and the unique feature of level attraction in dissipative coupling, i.e., the repelled damping parameters of supermodes. Furthermore, we show that the enhancement factor in mode broadening is larger than that in mode splitting when the dissipatively coupled photonic molecule works in the strong-coupling regime. Therefore, our scheme may be useful to resolve smaller changes in mode broadening and improve the detection limit of lossy-nanoparticle sensing.

DOI: 10.1103/PhysRevA.108.033716

## I. INTRODUCTION

Single nanoparticle sensing with ultrahigh sensitivity is of critical importance for many applications, e.g., environmental monitoring and early stage diagnosis of diseases [1]. Optical microcavity holds great potential in a single nanoparticle sensor because of significant enhancement of light-matter interaction with their high quality factor and small mode volumes [2,3]. Generally, sensing mechanisms for detecting different types of nanoparticles with a whispering-gallery mode (WGM) optical microcavity include mode shift [4], mode splitting [5], and mode broadening [6–8]. For lossy nanoparticles, e.g., carbon nanotubes and gold nanorods, they may strongly absorb the probe light and cause a significant broadening in the linewidth of cavity mode, thus a mode broadening sensing mechanism will be quite appropriate [6–8]. The distinct advantage of a mode broadening sensing mechanism is that it is insensitive to the fluctuation of environment temperature or system instability and it also removes the requirement of narrow linewidth (i.e., ultrahigh quality factor), which may greatly reduce the experimental difficulty. In order to further improve the sensing sensitivity, considerable efforts have been made [9–14]. In Ref. [9], Jing *et al.* have shown that nanoparticle-induced mode splitting is significantly enhanced in a rotating WGM microcavity due to frequency shifts from the Sagnac effect. In Ref. [10], Wiersig has found that a single optical microcavity operating at non-Hermitian spectral degeneracies, i.e., exceptional points (EPs), is useful for enhancing mode splitting, which has already been demonstrated with a single WGM microcavity [13]. The enhancement of mode splitting stems from the complex-square-root topology near EPs for the non-Hermitian system and the unique feature of level repulsion in coherent coupling. Furthermore, Chen *et al.* have shown that parity-time symmetric WGM microcavities operating at EPs can also exhibit larger mode splitting than the conventional sensors with a single microcavity [14]. To the best of our knowledge, most of the existing sensing enhancement schemes only focus on mode splitting [10–14], but the enhancement of mode broadening for lossy-nanoparticle sensing has not been studied yet. Considering the distinct advantage of mode broadening in lossy-nanoparticle sensing, it may be valuable to investigate the enhancement mechanism of mode broadening for the potential application of the WGM sensor. Unfortunately, we find that the enhancement of mode broadening for lossy-nanoparticle sensing may not be realizable with parity-time symmetric or coherently coupled microcavities directly as that in Ref. [14]; therefore, it is highly desirable to study this issue with other types of coupled microcavities.

Coupled microcavities are usually named as photonic molecules because the formation of optical supermodes are analogous to the electronic states in molecules formed by atoms [15]. Because of the additional degrees of freedom to tailor the optical density of states and the spatial distribution

*raul121991@126.com
†lmkuang@hunnu.edu.cn

 

of modes, the photonic molecule has been especially attractive for fundamental studies and practical applications, e.g., single-mode lasing [16], biosensor [17], and parity-time symmetry [18,19]. Generally, the photonic molecule may be formed in two different ways—the directly coupled geometry [15] and the indirectly coupled geometry (e.g., by waveguide [20–22], microcavity [23], or multilevel atom [24]). Up to now, a photonic molecule in the directly coupled geometry has been well studied, whereas the indirectly coupled geometry has not been effectively explored due to the lack of special utility. Recently, it has been shown that the coupling in the indirectly coupled geometry is tunable from traditional coherent coupling to dissipative coupling by the propagating phase [21,22] or frequency detuning [23]. Dissipative coupling has attracted great interest in an optomechanical system [25], plasmonic nanostructure [26], and cavity spintronics [27]. Especially, dissipative photon-magnon coupling has been demonstrated to be responsible for level attraction [27], nonreciprocity and unidirectional invisibility of microwave propagation [28], and steady Bell state generation [29]. Therefore, it may be of great importance to explore the new functionalities and deeply understand the existing phenomena with the dissipatively coupled photonic molecule in the indirectly coupled geometry.

Inspired by Refs. [10–14,23], we propose a feasible scheme for realizing a single-lossy-nanoparticle sensor with a dissipatively coupled photonic molecule and show that the significant enhancement of mode broadening can be obtainable at EPs when compared with a single WGM microcavity sensor subject to the same perturbation. The enhancement of mode broadening originates from the complex-square-root topology near EPs and the unique feature of level attraction in dissipative coupling, i.e., the repelled damping parameters of supermodes. On the other hand, we show that the strong dissipative coupling of the photonic molecule cannot be reachable directly [23], which hinders its potential application in the nanoparticle sensing. To overcome this difficulty, we consider asymmetric coupling of microcavities, impose the gain to suppress the additional loss in the microcavity, and show that strong dissipative coupling may be attainable. Benefitting from the strong dissipative coupling, we show that the enhancement factor in mode broadening is larger than that in mode splitting [14]; thus our scheme may be useful to resolve smaller changes in mode broadening and improve the detection limit of lossy-nanoparticle sensing.

## II. DISSIPATIVELY COUPLED PHOTONIC MOLECULE

The schematic diagram for the dissipatively coupled photonic molecule is illustrated in Fig. 1, where the active WGM microcavity $\mu R_1$ with the gain $\xi$ and the passive WGM microcavity $\mu R_2$ are both evanescently coupled to the highly dissipative WGM microcavity $\mu R_3$ with the strength $\kappa_{13}$ and $\kappa_{23}$, respectively. For simplicity, we only consider one of two modes $a_j$ (clockwise or counterclockwise), i.e., single-mode approximation, in $j$th ($j = 1, 2, 3$) microcavity with the eigenfrequency $\omega_j^0$ and the intrinsic loss $\gamma_j^0$ and then will take the effect of backscattering into account in Sec. III. By defining the complex frequencies $\omega_1' = \omega_1^0 + i(\xi - \gamma_1^0)/2$ and $\omega_j' = \omega_j^0 - i\gamma_j^0/2$ ($j = 2, 3$), we could denote the Hamiltonian of the system as $H = H_0 + V$ with ($\hbar = 1$)

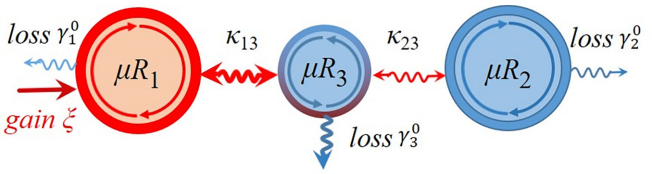


FIG. 1. Schematic diagram of dissipatively coupled photonic molecule. Active WGM microcavity $\mu R_1$ and passive WGM microcavity $\mu R_2$ are indirectly coupled by the highly dissipative WGM microcavity $\mu R_3$.

$$H_0 = \sum_{j=1}^{3} \omega_i' a_j^\dagger a_j, \quad V = (\kappa_{13} a_1^\dagger a_3 + \kappa_{23} a_2^\dagger a_3 + \text{H.c.}). \tag{1}$$

Due to the high loss of microcavity $\mu R_3$, i.e., $\gamma_3^0 \gg (\gamma_1^0, \gamma_2^0)$, we can adiabatically eliminate its mode using the Schrieffer-Wolff transformation by defining the generator as follows [30]:

$$S = \frac{\kappa_{13}}{\omega_1' - \omega_3'}(a_1^\dagger a_3 - a_3^\dagger a_1) + \frac{\kappa_{23}}{\omega_3' - \omega_2'}(a_3^\dagger a_2 - a_2^\dagger a_3). \tag{2}$$

It is straightforward to justify the identity $V + [S, H_0] = 0$, and hence the effective Hamiltonian can be written as

$$\begin{aligned} H_{\text{eff}} &= e^S H e^{-S} \approx H_0 + \frac{1}{2}[S, V] \\ &= \sum_{j=1,2} \left(\omega_j - i\frac{\gamma_j}{2}\right) a_j^\dagger a_j + \kappa_{12}(a_1^\dagger a_2 + a_2^\dagger a_1). \end{aligned} \tag{3}$$

As the microcavity $\mu R_3$ is decoupled with others, we have discarded its effect to the dynamical evolution of the system and hence obtain the indirectly coupled photonic molecule with the strength $\kappa_{12}$. The renormalized eigenfrequencies, loss rates, and the effective coupling between microcavity modes $a_1$ and $a_2$ are

$$\omega_j - i\frac{\gamma_j}{2} = \omega_j' + \frac{\kappa_{j3}^2}{\omega_j' - \omega_3'}, \tag{4}$$

$$\kappa_{12} = \frac{\kappa_{13}\kappa_{23}}{2}\left(\frac{1}{\omega_1' - \omega_3'} + \frac{1}{\omega_2' - \omega_3'}\right). \tag{5}$$

Evidently, the decoupling of dissipative mode $a_3$ also modifies the eigenfrequencies of modes $a_1$ and $a_2$ with the additional loss, and the effective coupling $\kappa_{12}$ combines the features of both coherent coupling and dissipative coupling, which are still to be explored. If two microcavities $\mu R_1$ and $\mu R_2$ are identical, i.e., $\omega_1^0 = \omega_2^0$ and $\gamma_1^0 = \gamma_2^0$, we can simplify the effective coherent coupling as $\kappa_{12} = 2\kappa_{13}\kappa_{23}/(\omega_1^0 - \omega_3^0)$ for large detuning $\omega_j^0 - \omega_3^0 \gg \gamma_3^0 - \gamma_j^0$. On the other hand, their effective loss rates remain unchanged as $\gamma_1 = \gamma_1^0 - \xi$ and $\gamma_2 = \gamma_2^0$ according to Eq. (4). If the following parameters $\kappa_{13} = \kappa_{23} \approx \omega_1^0 - \omega_3^0 \approx 10\gamma_3^0 \approx 50\gamma_1^0 \approx 50\gamma_2^0$ are satisfied, the strong coherent coupling $\kappa_{12} \approx 50\gamma_1 \approx 50\gamma_2$ will be realizable, which is consistent with the result in the cavity quantum electrodynamics system [31].

On the other hand, if the frequency detunings of three microcavities are far less than the corresponding intrinsic

loss detunings $\omega_j^0 - \omega_3^0 \ll \gamma_3^0 - \gamma_j^0$, the effective loss rates and coupling strength can be approximately expressed as

$$\gamma_1 = \gamma_1^0 - \xi + \frac{4\kappa_{13}^2}{\gamma_3^0 - \gamma_1^0 + \xi}, \quad \gamma_2 = \gamma_2^0 + \frac{4\kappa_{23}^2}{\gamma_3^0 - \gamma_2^0}, \tag{6}$$

$$\kappa_{12} = 2\kappa_{13}\kappa_{23}\left(\frac{1}{\gamma_3^0 - \gamma_1^0 + \xi} + \frac{1}{\gamma_3^0 - \gamma_2^0}\right)i. \tag{7}$$

To clearly analyze the dissipative coupling feature of the system, we discuss the cases with and without the gain in the microcavity $\mu R_1$, respectively. First, we consider the case of zero gain as Ref. [23] and the additional loss will dominate the decay of microcavities for the strong-coupling regime $(\kappa_{13}, \kappa_{23}, \gamma_3^0) \gg (\gamma_1^0, \gamma_2^0)$; thereby we can derive the ratios of effective coupling strength to the loss rates as

$$\frac{|\kappa_{12}|}{\gamma_1} \approx \frac{\kappa_{23}}{2\kappa_{13}}, \quad \frac{|\kappa_{12}|}{\gamma_2} \approx \frac{\kappa_{13}}{2\kappa_{23}}. \tag{8}$$

Therefore, it is impossible to simultaneously realize the strong coupling for microcavities $\mu R_1$ and $\mu R_2$ ($|\kappa_{12}| \gg \gamma_1$, $|\kappa_{12}| \gg \gamma_2$) regardless of the choice of the coupling strength $\kappa_{13}$ and $\kappa_{23}$.

However, the situation will be significantly changed for the existence of gain in the active microcavity $\mu R_1$. According to Eq. (7), the amplitude of effective coupling decreases slightly with the increase of gain, but the loss of the microcavity $\mu R_2$ remains unchanged as shown in the second term of Eq. (6); thus the asymmetric coupling of microcavities $\mu R_1$ and $\mu R_2$ with microcavity $\mu R_3$ ($\kappa_{13} \gg \kappa_{23}$) could lead to the strong coupling of the microcavity $\mu R_2$, i.e., $|\kappa_{12}|/\gamma_2 \sim \kappa_{13}/\kappa_{23} \gg 1$. On the other hand, the loss of the microcavity $\mu R_1$ can be greatly suppressed because of the gain as shown in the first term of Eq. (6) and it may also approach the strong-coupling regime $|\kappa_{12}| \gg \gamma_1$ in principle. If we choose the parameters of systems $\kappa_{13} = 10\kappa_{23}$ and $\kappa_{13} = \gamma_3^0 = \xi/1.56$, the ratios of effective coupling strength to loss of microcavities $\mu R_1$ and $\mu R_2$ will be $|\kappa_{12}|/\gamma_1 \approx 10$ and $|\kappa_{12}|/\gamma_2 \approx 4$, respectively. The key elements for realizing strong dissipative coupling are the ultralow loss of microcavity $\mu R_1$ suppressed by the gain and the asymmetric coupling of two microcavities, which provides an alternative platform for studying the related issues of the dissipatively coupled photonic molecule.

We now analyze the symmetry of the dissipatively coupled photonic molecule in the context of space-reversal and time-reversal operations, where parity operator means the exchange of modes $a_1$ and $a_2$ and time-reversal operator corresponds to complex conjugate. In the rotating frame of $\frac{1}{2}\sum_{j=1,2}(\omega_1 + \omega_2)a_j^\dagger a_j$, the effective Hamiltonian of dissipatively coupled photonic molecule $H_{\text{eff}}$ is just antiparity time symmetric for the identical loss rates $\gamma_1 = \gamma_2 = \gamma$ [22]. On the other hand, we solve the eigenequation $\det(H_{\text{eff}} - \omega I) = 0$ in the basis of $\{a_1, a_2\}$ and then obtain the eigenfrequencies of two supermodes as follows:

$$\omega_\pm = \frac{1}{4}\sum_{j=1}^{2}(2\omega_j - i\gamma_j) \pm \frac{1}{2}\sqrt{[2\omega_1 - 2\omega_2 - i(\gamma_1 - \gamma_2)]^2 + 4\kappa_{12}^2}. \tag{9}$$

We investigate the feature of its energy level by plotting the energy difference $\omega_\pm - \omega_1$ against the frequency detuning $\omega_2 - \omega_1$ in Fig. 2. For coherent coupling, we can see that the eigenfrequencies $\text{Re}(\omega_+)$ (black solid line) and $\text{Re}(\omega_-)$ (red dashed line) are repelled, but the damping parameters $\text{Im}(\omega_+)$ (pink dotted line) and $\text{Im}(\omega_-)$ (blue dot-dashed line) are attracted in Fig. 2(a), which is known as level repulsion. The opposite, called level attraction [27], is true for dissipative coupling as shown in Fig. 2(b), and the damping parameters $\text{Im}(\omega_+)$ (pink dotted line) and $\text{Im}(\omega_-)$ (blue dot-dashed line) of supermodes are repelled, which is the key point for realizing a lossy-nanoparticle sensor. The feature of level repulsion in a coherently coupled photonic molecule has been employed for the enhancement of mode splitting [10–14], while the feature of level attraction in a dissipatively coupled photonic molecule may be useful for the enhancement of mode broadening, which will be discussed in the following section.

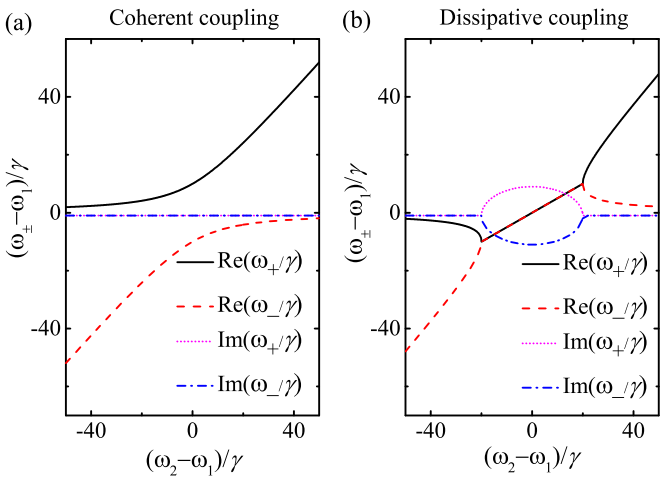


FIG. 2. (a) Level repulsion and (b) level attraction of the photonic molecule for coherent coupling and dissipative coupling, respectively. The parameters $|\kappa_{12}| = 10\gamma$ are taken into account.

## III. SINGLE-LOSSY-NANOPARTICLE SENSOR

In this section, we investigate a single-lossy-nanoparticle sensor with a dissipatively coupled photonic molecule, which is depicted in Fig. 3. We must point out that the following discussion of a lossy-nanoparticle sensor may be universal with a generally dissipatively coupled photonic molecule or dissipative backscattering in a single WGM microcavity [12], which may be not restricted to our scheme in Sec. II. By considering the clockwise (cw) and counterclockwise (ccw) modes in each WGM microcavity, we can express the

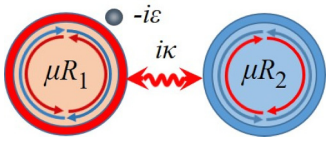


FIG. 3. Schematic diagram of single-lossy-nanoparticle sensor with dissipatively coupled photonic molecule, where $i\kappa$ is the strength of the dissipative coupling. The black sphere denotes the lossy nanoparticle with the perturbation strength $-i\varepsilon$.

Hamiltonian of a photonic molecule sensor as follows:

$$H_{s0} = \sum_{j=1,2}\sum_{l=1',2'}\left(\omega_j - i\frac{\gamma_j}{2}\right)a_{jl}^{\dagger}a_{jl} + \sum_{j,j'=1,2}^{j\neq j'}\sum_{l,l'=1',2'}^{l\neq l'} i\kappa a_{jl}^{\dagger}a_{j'l'}. \tag{10}$$

$a_{jl}^{\dagger}, a_{jl}$ are the creation and annihilation operators of $l$ mode in $j(j')$th WGM microcavity where $1'(2')$ stands for cw (ccw) and $\kappa$ is the strength of dissipative coupling. Without loss of generality, we assume that a lossy nanoparticle is introduced into the mode volume of microcavity $\mu R_1$ and it may induce the absorption loss and scattering loss of the cavity mode. To reveal the enhancement mechanism of mode broadening, we assume that the lossy-nanoparticle-induced backscattering and forward scattering is negligible; thus the main contribution is the absorption loss [7], which can be labeled with perturbation strength $-i\varepsilon(\varepsilon > 0)$. The perturbation Hamiltonian of the single lossy nanoparticle can be given by

$$H_{s1} = -i\varepsilon\sum_{l,l'=1',2'} a_{1l}^{\dagger}a_{1l'}. \tag{11}$$

Thus the total Hamiltonian is $H = H_{s0} + H_{s1}$ and we can obtain the corresponding eigenfrequencies by solving the eigenequation $\det(H - \omega I) = 0$ in the basis of $\{a_{11'}, a_{12'}, a_{21'}, a_{22'}\}$. If the loss rates of two WGM microcavities are identical, i.e., $\gamma_1 = \gamma_2 = \gamma$, the eigenfrequencies of supermodes can be expressed as follows:

$$\omega_{1\pm} = \frac{(\omega_1 + \omega_2)}{2} - i\frac{\gamma}{2} - i\varepsilon \pm \sqrt{\frac{(\omega_1 - \omega_2 - 2i\varepsilon)^2}{4} - \kappa^2}, \tag{12}$$

$$\omega_{2\pm} = \frac{(\omega_1 + \omega_2)}{2} - i\frac{\gamma}{2} \pm \sqrt{\frac{(\omega_1 - \omega_2)^2}{4} - \kappa^2}. \tag{13}$$

From Eqs. (12) and (13), we see that the incoming lossy nanoparticle lifts the eigenfrequency degeneracy of the supermodes: two supermodes experience both a frequency shift and linewidth broadening, whereas the other two supermodes are not affected and can serve as reference signals. Here, we may define the sensing sensitivity as mode broadening of a supermode relative to its reference signal $\mathrm{Im}(\Delta\omega_{\pm})$=$\mathrm{Im}(\omega_{1\pm} - \omega_{2\pm})$. From Eqs. (12) and (13) we can obtain

$$\Delta\omega_{\pm} = -i\varepsilon \pm \left(\sqrt{(\kappa_c - i\varepsilon)^2 - \kappa^2} - \sqrt{\kappa_c^2 - \kappa^2}\right), \tag{14}$$

where the critical coupling strength can be obtained from Eq. (13) with the expression $\kappa_c = |\omega_1 - \omega_2|/2$.

For a single WGM microcavity sensor with the same perturbation, we can derive the eigenfrequencies of two supermodes from Eq. (12) by setting $\kappa = 0$ and then obtain $\Delta\omega_{\mathrm{single}} = -i2\varepsilon$, which is just linear dependence of mode broadening on the perturbation strength. Here, we thus define an enhancement factor of mode broadening as follows:

$$\eta_{\pm} = \left|\frac{\mathrm{Im}(\Delta\omega_{\pm})}{\mathrm{Im}(\Delta\omega_{\mathrm{single}})}\right|, \tag{15}$$

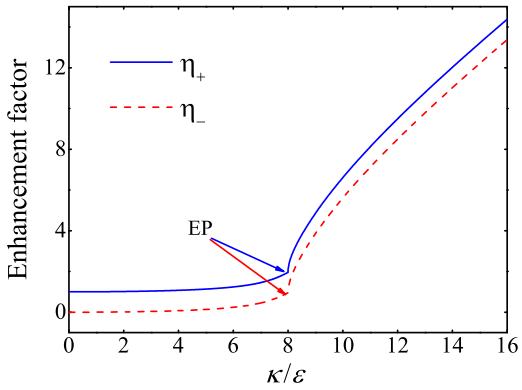


FIG. 4. Enhancement factor $\eta_+$ (blue solid line) and $\eta_-$ (red dashed line) of mode broadening versus the coupling strength of dissipatively coupled photonic molecule. The critical coupling strength is set as $\kappa_c = 8\varepsilon$.

which can be explicitly calculated with the following expression:

$$\eta_{\pm} = \tfrac{1}{2}\left|1 \mp \mathrm{Im}\left[\sqrt{(\kappa_c - i\varepsilon)^2 - \kappa^2} - \sqrt{\kappa_c^2 - \kappa^2}\right]/\varepsilon\right|. \tag{16}$$

We now can numerically analyze the influence of the coupling strength $\kappa$ on the enhancement factor of mode broadening $\eta_{\pm}$ based on Eq. (16). In Fig. 4, we plot the enhancement factors $\eta_+$ (blue solid line) and $\eta_-$ (red dashed line) with respect to the coupling strength of the dissipatively coupled photonic molecule when $\kappa_c = 8\varepsilon$. From Fig. 4, we can see that the enhancement factor of mode broadening exhibits a sudden change in the nearby EP regime. Especially, the enhancement factor can significantly increase in the regime of $\kappa > \kappa_c$.

For the non-Hermitian or anti-parity-time-symmetric system, we are interested in the feature of the square-root topology of the complex energy eigensurface at EPs [10–14]. We can exactly obtain the enhancement factor of mode broadening for the sensor operating at EPs $\kappa = \kappa_c$ with the simple expression

$$\Delta\omega_{\mathrm{EP}} = -i\varepsilon \pm \sqrt{-i\varepsilon(\omega_1 - \omega_2) - \varepsilon^2}. \tag{17}$$

When the lossy nanoparticle is sufficiently small, i.e., $\varepsilon \ll \kappa_c$, we can find $\mathrm{Im}(\Delta\omega_{\mathrm{EP}}) \approx -\sqrt{\kappa_c\varepsilon}$ and it shows the square-root dependence of mode broadening on the perturbation strength $\varepsilon$ at EPs, which may be universal for the non-Hermitian system at EPs [10–14].

As the lossy nanoparticle is small enough, the enhancement factor $\eta_{\pm} \approx \sqrt{\kappa_c/(4\varepsilon)}$ may be sufficiently large in the strong-coupling regime of photonic molecule $\kappa_c \gg \varepsilon$. It may be pointed out that if a lossy nanoparticle is introduced into the parity-time symmetric WGM photonic molecule, we can calculate its mode broadening $\mathrm{Im}(\Delta\omega'_{\mathrm{EP}}) = \mathrm{Im}(-i\varepsilon \pm \sqrt{|\gamma|\varepsilon}) = -\varepsilon$ based on Ref. [14]. Therefore, the enhancement of mode broadening for lossy-nanoparticle sensing may not be realizable with the parity-time symmetric WGM photonic molecule directly as that in Ref. [14]. On the other hand, the enhancement factor $\eta_{\pm}$ in mode broadening is also larger than that $[\eta_{\pm} = \sqrt{|\gamma|/(8\varepsilon)}]$ in mode splitting for the same perturbation strength such that the strong-coupling condition $\kappa_c \gg \gamma$ could be satisfied [14]. In order to intuitively show

TABLE I. Sensing sensitivity and enhancement factor for different sensing mechanisms.

| | Mode splitting $\mathrm{Re}(\Delta\omega_{\mathrm{EP}})$ | Mode broadening $\mathrm{Im}(\Delta\omega_{\mathrm{EP}})$ |
|---|---|---|
| Single microcavity | $2\varepsilon$ | $-2\varepsilon$ |
| Photonic molecule | $\sqrt{\lvert\gamma\rvert\varepsilon/2}$ Ref. [14] | $-\sqrt{\kappa_c\varepsilon}$ |
| Enhancement factor | $\sqrt{\lvert\gamma\rvert/(8\varepsilon)}$ Ref. [14] | $\sqrt{\kappa_c/(4\varepsilon)}$ |

the advantage of our scheme, we have summarized the sensing sensitivity and enhancement factor for different sensing mechanisms in Table I.

## IV. EXPERIMENTAL FEASIBILITY AND CONCLUSION

We briefly discuss the feasibility of our sensing scheme based on the experimentally accessible technology. First, we analyze the potential construction of a lossy-nanoparticle sensor, i.e., dissipatively coupled photonic molecule. Experimentally, each WGM microcavity may be readily constructed with microtoroid [18] and their eigenfrequencies can be tuned with a microheater for thermal tuning [32]. The coupling strength between microtoroids may be tunable with the precise manipulation of their relative distance, in which the nanopositioning systems are indispensable [18,32]. To be concrete, three microtoroids can be fabricated at the edges of separate chips placed on nanopositioning systems. Using a 10 nm step-resolution piezoelectric stage, each microtoroid can be held on the nanopositioning systems that could be manipulated relative to each other; thus the distance and hence the coupling strengths $\kappa_{13}$ and $\kappa_{23}$ can be precisely controlled [18]. The loss of microcavity $\mu R_3$ may be induced by a chromium-coated silica-nanofiber tip such that the highly dissipative condition $\gamma_3^0 \gg (\gamma_1^0, \gamma_2^0)$ can be reachable [33]. On the other hand, the active microcavity $\mu R_1$ can be fabricated from silica with $Er^{3+}$ dopants and its gain $\xi$ is adjustable with the power of pump laser [18,34]; thus the loss of the microcavity $\mu R_1$ can be greatly suppressed. Therefore, the required experimental platform for constructing a lossy-nanoparticle sensor can be realizable with the experimentally accessible technology [18,32,34]. It must be pointed out that for the sake of enhancing mode broadening the accurate manipulation of the coupling strengths $\kappa_{13}$ and $\kappa_{23}$, gain $\xi$ and loss $\gamma_3^0$ in the coupled microcavities is required, which may increase the experimental difficulty in contrast to the schemes with a single microcavity.

To discuss the performance of our lossy-nanoparticle sensor, we can choose a 13 nm × 5 nm gold nanorod as the analyte and the induced linewidth change for a single WGM microcavity is about 4.05 MHz, which corresponds to the perturbation strength of about $\varepsilon = 2.03$ MHz [8]. However, the experimental parameters, e.g., the quality factor of microcavities and the wavelength of probe laser, in coupled microcavities [18,33] are not consistent with those in mode broadening sensing for lossy nanoparticles [8]. Nevertheless, the coupling strength of microcavities, e.g., $\kappa_c \approx 16$ MHz, which is far larger than the perturbation strength $\varepsilon$ [18,33], can still be reachable; then the enhancement factor of 1.40 for mode broadening is obtainable. In Ref. [13], the enhancement factor of 2 for mode splitting has been realized at EPs of a single microcavity with the perturbation strength of about $\varepsilon = 5$ MHz. By considering the same perturbation strength for absorption loss and loss rate of microcavity $\mu R_1$ as Ref. [13], we can theoretically obtain the enhancement factor of 5.6 for mode broadening in the strong-coupling regime $\kappa_c = 4\gamma$.

In conclusion, we have proposed a feasible scheme for realizing a single-lossy-nanoparticle sensor with a dissipatively coupled WGM photonic molecule. It has been shown that the square-root dependence of mode broadening on the perturbation strength and significant enhancement in mode broadening can be obtainable at EPs when compared with a single WGM microcavity sensor subject to the same perturbation. The enhancement of mode broadening originates from the complex-square-root topology near EPs and the unique feature of level attraction in dissipative coupling and we show that the enhancement factor in mode broadening is larger than that in mode splitting when the dissipatively coupled photonic molecule works in the strong-coupling regime. Our scheme may be of great importance in not only the sensitivity enhancement mechanism but also the practical application of lossy-nanoparticle detection with a WGM sensor. In the future, it may be useful to resolve smaller changes in mode broadening and improve the detection limit of lossy-nanoparticle sensing.

## ACKNOWLEDGMENTS

Z.-H.P. and C.-X.J. were supported by the National Natural Science Foundation of China (NSFC) (Grant No. 11405052), the Natural Science Foundation of Hunan Province (Grant No. 2020JJ4286), and the Scientific Research Fund of Hunan Provincial Education Department (Grant No. 20C0785). Y.-Q.Z. was supported by NSFC (Grants No. 11504104 and No. 11704115). Y.Y. was supported by NSFC under Grant No. 12105097 and the Scientific Research Fund of Hunan Provincial Education Department (Grant No. 20C0787). L.-M.K. was supported by NSFC (Grants No. 12247105, No. 1217050862, and No. 11935006) and the Science and Technology Innovation Program of Hunan Province (Grant No. 2021RC2078).

[1] X. Fan, *Advanced Photonic Structures for Biological and Chemical Detection* (Springer, New York, 2009).
[2] X. Jiang, A. J. Qavi, S. H. Huang, and L. Yang, Matter **3**, 371 (2020).
[3] Y. Zhi, X. C. Yu, Q. Gong, L. Yang, and Y. F. Xiao, Adv. Mater. **29**, 1604920 (2017).
[4] F. Vollmer and S. Arnold, Nat. Methods **5**, 591 (2008).
[5] J. Zhu, S. K. Özdemir, Y. F. Xiao, L. Li, L. He, D. R. Chen, and L. Yang, Nat. Photon. **4**, 46 (2010).
[6] L. Shao, X. F. Jiang, X. C. Yu, B. B. Li, W. R. Clements, F. Vollmer, W. Wang, Y. F. Xiao, and Q. Gong, Adv. Mater. **25**, 5616 (2013).

[7] Y. Hu, L. Shao, S. Arnold, Y. C. Liu, C. Y. Ma, and Y. F. Xiao, Phys. Rev. A **90**, 043847 (2014).
[8] B. Q. Shen, X. C. Yu, Y. Zhi, L. Wang, D. Kim, Q. Gong, and Y. F. Xiao, Phys. Rev. Appl. **5**, 024011 (2016).
[9] H. Jing, H. Lü, S. K. Özdemir, T. Carmon, and F. Nori, Optica **5**, 1424 (2018).
[10] J. Wiersig, Phys. Rev. Lett. **112**, 203901 (2014).
[11] J. Wiersig, Phys. Rev. A **93**, 033809 (2016).
[12] J. Wiersig, Photon. Res. **8**, 1457 (2020).
[13] W. Chen, S. K. Özdemir, G. Zhao, J. Wiersig, and L. Yang, Nature (London) **548**, 192 (2017).
[14] W. Chen, J. Zhang, B. Peng, S. K. Özdemir, X. Fan, and L. Yang, Photon. Res. **6**, A23 (2018).
[15] K. Liao, X. Hu, T. Gan, Q. Liu, Z. Wu, C. Fan, X. Feng, C. Lu, Y. C. Liu, and Q. Gong, Adv. Opt. Photon. **12**, 60 (2020).
[16] T. Grossmann, T. Wienhold, U. Bog, T. Beck, C. Friedmann, H. Kalt, and T. Mappes, Light: Sci. Appl. **2**, e82 (2013).
[17] S. V. Boriskina and L. D. Negro, Opt. Lett. **35**, 2496 (2010).
[18] B. Peng, S. K. Özdemir, F. Lei, F. Monifi, M. Gianfreda, G. L. Long, S. Fan, F. Nori, C. M. Bender, and L. Yang, Nat. Phys. **10**, 394 (2014).
[19] L. Chang, X. Jiang, S. Hua, C. Yang, J. Wen, L. Jiang, G. Li, G. Wang, and M. Xiao, Nat. Photon. **8**, 524 (2014).
[20] M. F. Yanik, W. Suh, Z. Wang, and S. Fan, Phys. Rev. Lett. **93**, 233903 (2004).
[21] Y. F. Xiao, M. Li, Y. C. Liu, Y. Li, X. Sun, and Q. Gong, Phys. Rev. A **82**, 065804 (2010).
[22] Z. H. Peng, C. X. Jia, Y. Q. Zhang, J. B. Yuan, and L. M. Kuang, Phys. Rev. A **102**, 043527 (2020).
[23] W. Yu, J. Wang, H. Y. Yuan, and J. Xiao, Phys. Rev. Lett. **123**, 227201 (2019).
[24] S. I. Schmid and J. Evers, Phys. Rev. A **84**, 053822 (2011).
[25] N. R. Bernier, L. D. Toth, A. K. Feofanov, and T. J. Kippenberg, Phys. Rev. A **98**, 023841 (2018).
[26] Q. H. Song and H. Cao, Phys. Rev. Lett. **105**, 053902 (2010).
[27] M. Harder, Y. Yang, B. M. Yao, C. H. Yu, J. W. Rao, Y. S. Gui, R. L. Stamps, and C. M. Hu, Phys. Rev. Lett. **121**, 137203 (2018).
[28] Y. P. Wang, J. W. Rao, Y. Yang, P. C. Xu, Y. S. Gui, B. M. Yao, J. Q. You, and C. M. Hu, Phys. Rev. Lett. **123**, 127202 (2019).
[29] H. Y. Yuan, P. Yan, S. Zheng, Q. Y. He, K. Xia, and M. H. Yung, Phys. Rev. Lett. **124**, 053602 (2020).
[30] J. R. Schrieffer and P. A. Wolff, Phys. Rev. **149**, 491 (1966).
[31] Y. C. Liu, X. Luan, H. K. Li, Q. Gong, C. W. Wong, and Y. F. Xiao, Phys. Rev. Lett. **112**, 213602 (2014).
[32] H. Rokhsari and K. J. Vahala, Phys. Rev. Lett. **92**, 253905 (2004).
[33] B. Peng, S. K. Özdemir, S. Rotter, H. Yilmaz, M. Liertzer, F. Monifi, C. M. Bender, F. Nori, and L. Yang, Science **346**, 328 (2014).
[34] L. He, S. K. Özdemir, and L. Yang, Laser Photon. Rev. **7**, 60 (2013).